Orientation-Selective ESEEM Study and Crystal Structure of a Cu^{II}(thiochrome)Cl_2 Complex

Maria Louloudi,[†] Yiannis Deligiannakis,[‡] Jean-Pierre Tuchagues,[§] Bruno Donnadieu,[§] and Nick Hadjiliadis*,[†]

Department of Chemistry, University of Ioannina, Ioannina 45110, Greece, Institute of Materials Science, NCSR Demokritos, Agia Paraskevi, Attiki 15310, Greece, and Laboratoire de Chimie de Coordination du CNRS, 205 route de Narbonne, 31077 Toulouse Cedex, France

Received May 28, 1997[⊗]

The reaction of Cu(II) with 2-(α-hydroxybenzyl)thiamine in methanolic solutions produces Cu(I) and thiochrome. The crystal structure of the Cu^{II}(thiochrome)Cl_2 complex, formed from the reaction media, comprises an infinite array of Cu(thiochrome)Cl_2 neutral units linked together through the N(4′a) and N(1′) atoms of thiochrome, coordinated to Cu(II). The copper atom is tetracoordinated with a weak Cu···N(3′) interaction in a compressed tetrahedral environment. Crystallographic data: space group $P2_1$, $a = 7.433(1)$ Å, $b = 11.826(6)$ Å, $c = 10.009(2)$ Å, $\beta = 91.25(1)°$, $V = 879.7(5)$ Å^3, $Z = 2$. Continuous wave EPR spectroscopy shows that this conformation is retained in frozen solution. Magnetic susceptibility data in the 2−300 K temperature range showed that the μ_{eff}/Cu variation (1.68−1.74 μ_B) was negligible, indicating the absence of magnetic interactions between the Cu(II) ions. In Cu^{II}(thiochrome)Cl_2 the magnetic interaction between the N(3′) nitrogen of the pyrimidine ring and the copper $d_{x^2-y^2}$ electron spin is detected by ESEEM spectroscopy. The ESEEM data show the existence of a weak magnetic interaction ($A_x = 1.6$ MHz, $A_y = 1.4$ MHz, $A_z = 1.0$ MHz) between the Cu unpaired electron spin and the nucleus of the ^{14}N(3′) of the pyrimidine ring. The nuclear quadrupole parameters for the nitrogen ($e^2qQ/h = 3.1$ MHz, $\eta = 0.25$) differ from those in crystalline pyrimidine, and this is discussed in terms of the electron distribution on the pyrimidine ring in the Cu^{II}(thiochrome)Cl_2 complex. It is once more shown that the ESEEM technique can provide useful structural information on similar inorganic systems, in the absence of X-ray diffraction data.

Introduction

The active aldehyde derivatives of thiamine pyrophosphate (structure **I**) are intermediates formed during its enzymatic action. In the presence of a Mg(II) ion, thiamine pyrophosphate catalyzes the decarboxylation of α-keto acids and the transfer of aldehyde or acyl groups *in vivo*. Other bivalent metal ions like Co(II), Zn(II), Cd(II), and Ni(II) are also known to be active *in vitro*.[1]

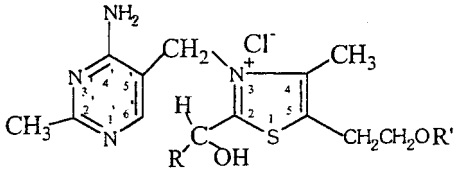

R: CH_3-, C_6H_5-, C_6H_{11}-

R': $HP_2O_6^{2-}$

Structure I

The active aldehyde derivatives of thiamine, 2-(α-hydroxybenzyl)- and 2-(α-hydroxy-α-cyclohexylmethyl)thiamine, form complexes with group IIB metals,[2] as well as first-row transition metals,[3] all coordinated to the N(1′) site of the pyrimidine moiety.

Our investigations on the interaction of metal ions with these active thiamine intermediates had also involved Cu(II).[3,4] The interest in this metal is due to the possible role that Cu(II) may have in the oxidation of thiamine and active aldehydes of thiamine to thiochrome. Previous attempts to prepare Cu(II)−thiamine complexes showed either no bonding between the Cu(II) ion and the ligand[5] or Cu(I)−thiamine and Cu(I)−thiochrome complexes.[6] A crystal structure of [(thiamine pyrophosphate)(1,10-phenanthroline)aquacopper(II)] demonstrated that the complex ion coordinated to the thiamine moiety only via the pyrophosphate group.[7]

Electron paramagnetic resonance (EPR) is a well-established technique for the study of the coordination geometry of Cu(II). Continuous wave (CW) EPR has been used extensively as a tool for the diagnosis of the coordination environment of Cu(II) complexes.[8] When the EPR spectrum is governed by anisotropic interactions, it is possible to perform orientation-selective ESEEM experiments.[9] When a ^{14}N nucleus is coupled with the electron spin, these experiments can provide the

* Author to whom correspondence may be addressed.
[†] Department of Chemistry, University of Ioannina.
[‡] Institute of Materials Science, NCSR Demokritos.
[§] Laboratoire de Chimie de Coordination du CNRS.
[⊗] Abstract published in *Advance ACS Abstracts,* November 15, 1997.

(1) Krampitz, L. O. *Annu. Rev. Biochem.* **1969**, *38*, 213.
(2) Louloudi, M.; Hadjiliadis, N.; Feng, J. A.; Sukumar, S.; Bau, R. J. *J. Am. Chem. Soc.* **1990**, *112*, 7233. (b) Dodi, K.; Gerothanassis, I.; Hadjiliadis, N.; Schreiber, A.; Bau, R.; Butler, I.; Barrie, P. *Inorg. Chem.* **1996**, *35*, 6513.
(3) Louloudi, M.; Hadjiliadis, N. *J. Chem. Soc., Dalton Trans.* **1992**, 1635.
(4) Louloudi, M.; Hadjiliadis, N.; Butler, I. S. *Can. J. Appl. Spectrosc.* **1994**, *39*, 31.
(5) Caira, M. R.; Fazakerley, G. V.; Linder, P. W.; Nassimbeni, L. R. *Acta Crystallogr.* **1974**, *B30*, 1660.
(6) Cramer, R. E.; Maynard, R. B.; Evangelista, R. S. *J. Am. Chem. Soc.* **1984**, *106*, 111. (b) Archibong, E.; Adeyemo, A.; Aoki, K.; Yamazaki, H. *Inorg. Chim. Acta* **1989**, *156*, 77. (c) Kitagawa, S.; Matsuyama, S.; Munakata, M.; Osawa, N.; Masuda, H. *J. Chem. Soc., Dalton Trans.* **1991**, 1717.
(7) Aoki, K.; Yamazaki, H. *J. Am. Chem. Soc.* **1980**, *102*, 6878.
(8) Hathaway, B. J.; Billing, D. E. *Coord. Chem. Rev.* **1970**, *5*, 143.

S0020-1669(97)00638-1 CCC: $14.00

orientation of the ^{14}N hyperfine and quadrupole tensors with respect to the **g** tensor, which in turn can be interpreted in terms of the complex conformation and bonding parameters.[9a−c,10]

In the past the pulsed-EPR technique of electron spin echo envelope modulation[11] (ESEEM) has been used in the study of metal binding sites of various Cu(II) protein complexes and in model compounds.[12] These studies provided important insight into the characterization of the local environment of the paramagnetic centers and the effect of local interactions, like H-bonding, on the coordination environment of the Cu(II).[13] The majority of these ESEEM studies were concentrated on Cu(II)−(histidine)$_n$ complexes, while reports of ESEEM work on Cu(II) with non-histidine ligands are scarce.

In this contribution we report the polymeric crystal structure of Cu(II)(thiochrome)Cl_2. In solution, Cu(II) reacts with 2-(α-hydroxybenzyl)thiamine to produce thiochrome. This structural report appears to be the first example of a Cu(II) complex of thiamine or its derivatives with a direct Cu(II)−N bond and only the second example of a thiamine or a thiamine derivative directly bonded to a Cu(II) ion. We have also studied the coordination environment of the Cu(II)−thiochrome by CW EPR and orientation-selective ESEEM spectroscopy. The ESEEM data are in agreement with the crystal structure and show that the N(3′) nitrogen of the pyrimidine ring is weakly coupled with the Cu(II) electron spin.

Experimental Section

Materials. Thiamine chloride hydrochloride was purchased from Sigma Chemical Co. and used without further purification. $CuCl_2$ and other chemicals used were from Aldrich AG. The ligand 2-(α-hydroxybenzyl)thiamine was prepared as described in the literature.[14]

Preparation of {Cu(thiochrome)Cl_2}$_n$ Crystals. A methanolic solution (25 mL, 10^{-2} M) of the ligand 2-(α-hydroxybenzyl)thiamine, neutralized following the procedure as described,[2a] and 25 mL of a 10^{-2} M methanolic solution of $CuCl_2$ were added separately into the different branches of a U-shaped tube, which were separated by a ceramic filter. The tube was left in a glovebox, and crystals of the compound {Cu(thiochrome)Cl_2}$_n$ suitable for X-ray analysis were obtained by slow mixing of the two solutions.

Methods. 1. Magnetic Susceptibility Studies. Variable temperature magnetic susceptibility data were obtained on powdered polycrystalline samples with a Quantum Design MPMS SQUID susceptometer. Diamagnetic corrections were applied by using Pascal's constants.

2.1. EPR and ESEEM Spectra. Continuous wave (CW) EPR spectra were recorded at liquid helium temperatures with a Bruker ER 200D X-band spectrometer equipped with an Oxford Instruments cryostat. The microwave frequency and the magnetic field were measured with a microwave frequency counter HP 5350B and a Bruker ER035M NMR gaussmeter, respectively. Pulsed EPR was performed with a Bruker ESP 380 spectrometer with a dielectric resonator.[15] In the three-pulse ($\pi/2-\tau-\pi/2-T-\pi/2$) ESEEM data, the amplitude of the stimulated echo as a function of $\tau + T$ was measured at a frequency near 9.6 GHz at a magnetic field corresponding to the maximum intensity of the field-swept spectrum. The minimum interpulse T was 32 ns and was incremented in steps of 8 ns; the duration of the $\pi/2$ pulse was 16 ns. Dead-time reconstruction was performed according to Mims.[16] To remove the unwanted echoes in a three-pulse experiment, the phase-cycling procedure was applied.[17] Before Fourier transformation the time domain echo decay was factored out by subtraction of a sixth-order polynomial. The field-swept spectra were obtained by recording the integral of the echo as a function of the magnetic field after a two-pulse sequence ($\pi/2-200$ ns$-\pi$); the durations of the $\pi/2$ and π pulses were 16 and 32 ns, respectively, and the integration gate was 200 ns.

2.2. ESEEM Simulations. A. ^{14}N ($S = {}^1/_2$, $I = 1$). The spin Hamiltonian for an $S = {}^1/_2$, $I = 1$ system expressed in the **g** tensor principal axis system is

$$H = (\beta/h)H\mathbf{g}S - g_N(\beta/h)HI + S\cdot\mathbf{A}'\cdot I + I\cdot\mathbf{Q}'\cdot I \qquad (1)$$

The tensor **g** has principal values (g_x, g_y, g_z), and the Euler angles α, β, and γ relate the principal axis system of the **A**′ and **g** tensors.[18] The Euler angles used are defined according to the convention of Margenau and Murphy.[18] The polar angles θ and ϕ determine the orientation of the applied magnetic field in the **g**-tensor principal axes according to standard notation. The hyperfine tensor **A**′ in eq 1 is defined as **A**′ = **Ag** where the diagonal values of the **A** tensor in its principal axis system are (A_{xx}, A_{yy}, A_{zz}). The Euler angles u, v, and w relate the principal axis systems of the nuclear quadrupole interaction **Q**′ and **g** tensors. The tensor **Q**′ in its principal axis system has diagonal values ($2K$, $-K[1-\eta]$, $-K[1+\eta]$) where K represents the quadrupole coupling constant $e^2qQ/4h$ and η is the asymmetry parameter of the electric field gradient. In the calculations we neglect the hyperfine and quadrupole interactions of the copper nucleus, which do not affect the ESEEM.[19a] The energies and eigenfunctions are calculated numerically for each spin manifold, and the three-pulse modulations E_α and E_β were calculated with the relations derived by Mims.[19b]

B. Orientation Selection. Due to the large **g** anisotropy and the limited microwave power of the microwave pulses in our experiment, at each resonant field only spins at certain orientations θ and ϕ contribute to the detected echo. The ranges of θ and ϕ that contribute the echo at each magnetic field within the EPR line shape were determined graphically as described by Golfarb et al.[9a] With the use of the parameters (g_x, g_y, g_z) and A_x(Cu), A_y(Cu), and A_z(Cu) as determined from the CW EPR spectrum, a plot of the resonant fields for each m_I (Cu) value as a function of θ was generated. Since the EPR spectrum of the Cu(thiocrome)Cl_2 complex is axial, the calculations were performed for $\phi = 0$. The orientation contributing to the echo intensity for each experimental resonant field was determined from this plot. A total line width of 40 G was taken, from which the integration region for θ was determined.

The total echo intensity was calculated from

$$E(\tau,T,H) = \int_0^{\pi}\int_{\theta_{min}}^{\theta_{max}}[E_\alpha(\tau,T,H,\theta,\phi) + E_\beta(\tau,T,H,\theta,\phi)]\sin\theta\,d\theta\,d\phi$$

Before Fourier transformation, the simulated spectra described above, after removal of the constant component, were convoluted with a Hamming function, like the experimental spectra. The frequency domain spectra are calculated in the Sqrt(Re^2+Im^2) mode.

3. X-ray Crystal Structure Determination of {Cu(thiochrome)Cl_2}$_n$. A dark-green platelet (0.51 × 0.30 × 0.05 mm) was sealed on

(9) Goldfarb, D.; Fauth, J.-M.; Tor, Y.; Shanzer, A. *J. Am. Chem. Soc.* **1991**, *113*, 1941. (b) Kofman, V.; Dikanov, S. A.; Haran, A.; Libman, J.; Shanzer, A.; Goldfarb, D. *J. Am. Chem. Soc.* **1995**, *117*, 383. (c) Flanagan, H. L.; Gerfen, G. J.; Lai, A.; Singel, D. J. *J. Chem. Phys.* **1988**, *88*, 2162.

(10) Dikanov, S. A.; Samoilova, R. I.; Smiega, J. A.; Bowman, M. K. *J. Am. Chem. Soc.* **1995**, *117*, 10579.

(11) Dikanov, S. A.; Tsvetkov, Y. D. *ESEEM spectroscopy*; CRC Press: Boca Raton, FL, 1992.

(12) Mondovi, B.; Morpugo, L.; Agonistelli, E.; Befani, O.; McCracken, J.; Peisach, J. *Eur. J. Biochem.* **1977**, *168*, 503. (b) Mims, W. B.; Peisach, J. *J. Biol. Chem.* **1979**, *254*, 4321. (c) Zweier, J. L.; Peisach, J.; Mims, W. B. *J. Biol. Chem.* **1982**, *257*, 10314. (d) McCracken, J.; Desai, P. R.; Papadopoulos, N. J.; Villafranca, J. J.; Peisach, J. *Biochemistry* **1988**, *27*, 4133. (e) Jiang, F.; Karlin, K. D.; Peisach, J. *Inorg. Chem.* **1993**, *32*, 2576.

(13) Jiang, F.; McCracken, J.; Peisach, J. *J. Am. Chem. Soc.* **1990**, *112*, 9035.

(14) Mieyal, J. J.; Bantle, G.; Votaw, R. G.; Rosner, J. A.; Sable, H. Z. *J. Biol. Chem.* **1971**, *246*, 5213.

(15) Deligiannakis, Y.; Boussac, A.; Rutherford, A. W. *Biochemistry* **1995**, *34*, 16030.

(16) Mims, W. B. *J. Magn. Reson.* **1984**, *59*, 291.

(17) Fauth, J. M.; Schweiger, A.; Braunschweiler, L.; Forrer, J.; Ernst, R. *J. Magn. Reson.* **1986**, *66*, 64.

(18) Margenau, H.; Murphy, J. M. *The Mathematics of Physics and Chemistry*; Van Nostrand Company Inc.: Princeton, NJ, 1957.

(19) Rowan, L. G.; Hahn, E. L.; Mims, W. B. *Phys. Rev. A* **1965**, *137*, 61. (b) Mims, W. B. *Phys. Rev. B.* **1972**.

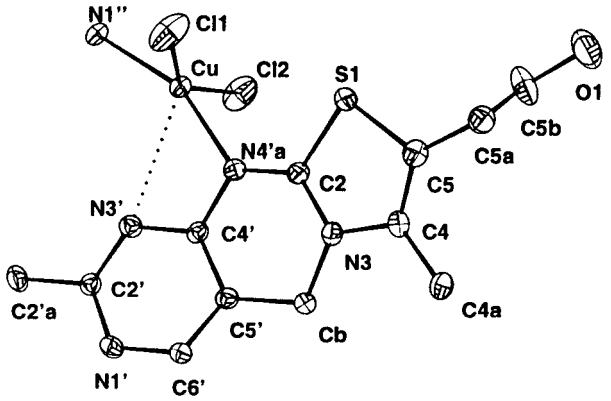

Figure 1. Crystal structure of Cu(thiochrome)Cl_2 complex (**1**).

Table 1. Crystallographic Data for $[Cu(C_{12}H_{13}N_4OS)Cl_2].CH_3OH$ (**1**)

empirical formula $CuC_{13}H_{17}N_4O_2SCl_2$	mol wt 427.8
space group $P2_1$ (No. 4)	$T = 20$ °C
$a = 7.433(1)$ Å	
$b = 11.826(6)$ Å	$\beta = 91.25(1)$ (deg)
$c = 10.009(2)$ Å	
$V = 879.7(5)$ Å^3	$\lambda = 0.710\ 73$ Å
$\rho_{calc} = 1.61$ g cm^{-3}	μ(Mo Kα) = 16.77 cm^{-1}
$Z = 2$	transm coeff = 0.95−1.07
$R = \sum(\|\|F_o\| - \|F_c\|\|)/\sum\|F_o\| = 0.030$	$R_w = [\sum(\|\|F_o\| - \|F_c\|\|)^2/\sum(\|F_o\|)^2]^{1/2} = 0.032$

a glass fiber and mounted on an Enraf-Nonius CAD 4 diffractometer, and 3102 reflections (1809 unique) with $2\theta \leq 54°$ were collected at 20 °C using Mo Ka radiation with a graphite monochromator (λ = 0.710 73 Å). The crystal of $[Cu(C_{12}H_{13}N_4OS)(Cl)_2]\cdot CH_3OH$ belongs to the monoclinic system, and its space group was assigned as $P2_1$ from extinctions $0k0$, $k = 2n + 1$. The crystal quality was monitored by scanning three standard reflections every 2 h. No significant variation was observed during data collection. After corrections for Lorentz and polarization effects,[20] an empirical absorption correction was applied.[21]

4. Structure Solution and Refinement. The structure was solved by using direct methods[22] and refined by full matrix least-squares.[23] All non-hydrogen atoms were refined anisotropically. All hydrogen atoms including those of methanol were found on difference Fourier synthesis and included in calculations with a constrained geometry (C−H = 0.98 Å). Hydrogen isotropic temperature factors were kept fixed 20% higher than those of the carbon atom to which the hydrogen was bonded. The atomic scattering factors and anomalous dispersion terms were taken from the standard compilation.[24] The final refinement cycle converged to $R = 0.030$ and $R_w = 0.032$ with a Chebyshev weighting scheme.[25] The goodness of fit was $s = 1.17$ with 1482 reflections ($I > 3\sigma(I)$) and 227 variable parameters. All calculations were performed on a PC using the programs SHELXS-86,[22] CRYSTALS,[23] and CAMERON.[26] The $[Cu(C_{12}H_{13}N_4OS)(Cl)_2]\cdot CH_3OH$ complex molecule is shown in Figure 1 with atom numbering. The crystallographic data are summarized in Table 1. Final fractional atomic coordinates with their estimated standard deviations and selected bond lengths and angles are given in Tables 2 and 3, respectively.

(20) Watkin, D. J.; Prout, C. K.; Lilley, P. M. Q. *RC93*; Chemical Crystallography Laboratory: oxford, U.K., 1994.
(21) Walker, N.; Stuart, D. *Acta Crystallogr., Sect. A: Found. Crystallogr.* **1983**, *39*, 158.
(22) Sheldrick, G. M. *SHELXS-86. Program for Crystal Structure Solution;* University of Göttingen; Göttingen, Germany, 1986.
(23) Watkin, D. J.; Prout, C. K.; Carruthers, R. J.; Betteridge, P. *Crystals*, Issue 10; Chemical Crystallography Laboratory, Oxford, U.K., 1996.
(24) *International Tables for X-ray Crystallography;* Kynoch Press: Birmingham, England, 1974; Vol. IV.
(25) Carruthers, J. R.; Watkin, D. J. *Acta Crystallogr., Sect. A: Found. Crystallogr.* **1979**, *35*, 698.
(26) Watkin, D. J.; Prout, C. K.; Pearce, L. K. *Cameron*; Chemical Crystallography Laboratory: Oxford, U.K., 1996.

Table 2. Fractional Atomic Coordinates and Isotropic Equivalent Temperature Factors (Å^2 × 100) with Esd's in Parentheses for $[Cu(C_{12}H_{13}N_4OS)Cl_2]\cdot CH_3OH$ (**1**)

atom	*x*/*a*	*y*/*b*	*z*/*c*	U_{eq}[a]
Cu	0.21298(7)	0.0002(1)	0.90911(5)	3.03
Cl(1)	0.4562(2)	0.0125(2)	1.0395(2)	6.18
Cl(2)	0.0761(3)	0.0474(2)	0.7117(2)	5.80
S(1)	0.5961(2)	−0.1109(1)	0.7381(1)	3.87
O(1)	0.9813(8)	−0.0950(6)	0.3855(5)	7.79
N(3)	0.4246(5)	−0.2947(3)	0.7202(4)	3.06
N(4′a)	0.2702(6)	−0.1522(4)	0.8418(4)	3.28
N(3′)	0.0214(6)	−0.1936(3)	0.9627(4)	3.10
N(1′)	−0.0791(6)	−0.3815(3)	0.9890(4)	3.12
C(5b)	0.8299(9)	−0.1247(8)	0.4588(7)	5.80
C(5a)	0.8614(8)	−0.2033(5)	0.5767(6)	4.33
C(5)	0.6915(8)	−0.2218(5)	0.6488(6)	3.31
C(4)	0.5821(7)	−0.3144(5)	0.6509(5)	3.54
C(4a)	0.6141(9)	−0.4266(5)	0.5899(7)	4.78
C(2)	0.4095(7)	−0.1902(4)	0.7706(5)	3.17
C(4′)	0.1470(7)	−0.2308(4)	0.8791(4)	2.75
C(5′)	0.1526(6)	−0.3446(4)	0.8367(5)	3.03
C(b)	0.2763(7)	−0.3771(4)	0.7268(5)	3.10
C(6′)	0.0396(7)	−0.4166(4)	0.8986(5)	3.15
C(2′)	−0.0904(7)	−0.2698(4)	1.0118(5)	2.94
C(2′a)	−0.2379(8)	−0.2272(5)	1.0970(6)	4.10
C(20)	0.223(1)	0.7162(9)	0.376(1)	7.27
O(2)	0.351(1)	0.729(1)	0.277(1)	17.46

[a] U_{eq} = one-third of the trace of the orthogonalized $\mathbf{U}_{ij}$ tensor.

Table 3. Selected Interatomic Distances (Å) and Angles (deg) for $[Cu(C_{12}H_{13}N_4OS)Cl_2]\cdot CH_3OH$ (**1**)[a]

Cu−Cl(1)	2.216(2)	Cu−Cl(2)	2.267(2)
Cu−N(4′a)	1.977(4)	Cu−N(1″)	2.004(4)
S(1)−C(5)	1.746(6)	S(1)−C(2)	1.711(5)
O(1)−C(5b)	1.401(8)	N(3)−C(4)	1.393(6)
N(3)−C(2)	1.340(6)	N(3)−C(b)	1.474(6)
N(4′a)−C(2)	1.347(6)	N(4′a)−C(4′)	1.363(6)
N(3′)−C(4′)	1.341(6)	N(3′)−C(2′)	1.328(6)
N(1′)−C(6′)	1.343(6)	N(1′)−C(2′)	1.344(7)
C(5b)−C(5a)	1.516(9)	C(5a)−C(5)	1.484(8)
C(5)−C(4)	1.365(8)	C(4)−C(4a)	1.482(8)
C(4′)−C(5′)	1.412(7)	C(5′)−C(b)	1.499(6)
C(5′)−C(6′)	1.355(7)	C(2′)−C(2′a)	1.490(7)
Cu−N(3′)	2.753(4)		
Cl(1)−Cu−Cl(2)	147.8(08)	Cl(1)−Cu−N(4′a)	94.5(1)
Cl(2)−Cu−N(4′a)	91.4(1)	Cl(1)−Cu−N(1″)	93.5(1)
Cl(2)−Cu−N(1″)	93.2(1)	N(4′a)−Cu−N(1″)	157.6(2)
C(5)−S(1)−C(2)	91.5(3)	C(4)−N(3)−C(2)	114.8(4)
C(4)−N(3)−C(b)	123.3(4)	C(2)−N(3)−C(b)	121.6(4)
Cu−N(4′a)−C(2)	131.4(3)	Cu−N(4′a)−C(4′)	112.1(3)
C(2)−N(4′a)−C(4′)	115.9(4)	C(4′)−N(3′)−C(2′)	117.2(4)
Cu−N(1″)−C(6′)	117.7(3)	Cu−N(1″)−C(2′)	124.5(3)
C(6′)−N(1′)−C(2′)	117.6(4)	O(1)−C(5b)−C(5a)	116.7(6)
C(5b)−C(5a)−C(5)	110.5(5)	S(1)−C(5)−C(5a)	119.8(4)
S(1)−C(5)−C(4)	110.3(4)	C(5a)−C(5)−C(4)	129.7(5)
N(3)−C(4)−C(5)	112.3(5)	N(3)−C(2)−C(4a)	119.9(5)
C(5)−C(4)−C(4a)	127.7(5)	S(1)−C(2)−N(3)	111.0(4)
S(1)−C(2)−N(4′a)	123.6(4)	N(3)−C(2)−N(4′a)	125.3(4)
N(4′a)−C(4′)−N(3′)	115.3(4)	N(4′a)−C(4′)−C(5′)	122.9(4)
N(3′)−C(4′)−C(5′)	121.8(4)	C(4′)−C(5′)−C(b)	119.2(4)
C(4′)−C(5′)−C(6′)	116.0(4)	C(b)−C(5′)−C(6′)	124.8(4)
N(3)−C(b)−C(5′)	109.5(4)	N(1′)−C(6′)−C(5′)	122.4(4)
N(3′)−C(2′)−N(1′)	124.3(5)	N(3′)−C(2′)−C(2′a)	117.2(5)
N(1′)−C(2′)−C(2′a)	118.6(4)	Cl(1)−Cu−N(3′)	110.9(1)
Cl(2)−Cu−N(3′)	98.8(1)	N(4′a)−Cu−N(3′)	54.8(1)
N(3′)−Cu−N(1″)	102.8(1)		

[a] Symmetry: Prime (′) and double prime (″) = $-x$, $y + {}^1/_2$, $-z$.

Results and Discussion

1. CW EPR Spectroscopy and Magnetic Susceptibility Studies. The EPR spectrum of the polycrystalline Cu(thiochrome)Cl_2 complex in toluene, Figure 3, is almost axial. The *g* values and hyperfine coupling parameters, *A*, were determined

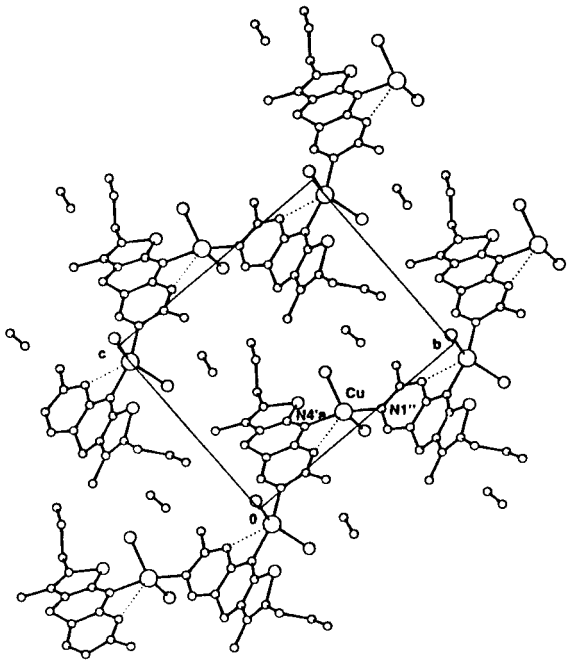

Figure 2. Projection along the *a* axis.

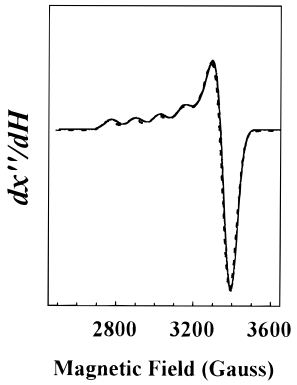

Figure 3. EPR spectrum of polycrystalline Cu(thiochrome)Cl_2 in toluene, at 45 K. EPR conditions: microwave frequency 9.42 GHz; microwave power 2 mW; modulation amplitude 10 G. The dashed trace represents computer simulations obtained with the parameters given in Table 4.

Table 4. *g* and *A*(Cu) (MHz) values of Cu(thiochrome)Cl_2

g_{xx}	g_{yy}	g_{zz}	A_{xx}	A_{yy}	A_{zz}
2.06	2.06	2.31	55	55	380

from the numerical simulation of the spectrum (Figure 3 dotted line) and are listed in Table 4. The line width in the spectrum of the frozen sample is found to be anisotropic. Any superhyperfine splitting due to the ligand nuclear spins or an isotope effect due to the occurrence of ^{63}Cu and ^{65}Cu cannot be resolved in the experimental spectrum. Thus these effects are included in the line width in the simulations.

In general the parallel components of the spin Hamiltonian for Cu(II) complexes, $g_{||}$ and $A_{||}$, can be determined more reliably than the perpendicular components, $g_\perp$ and $A_\perp$. The fact that the complex Cu(thiochrome)Cl_2 is characterized by $g_{||} < g_\perp$ is indicative of a $d_{x^2-y^2}$ ground state.[27] The nondegenerate ground state might be due to the low symmetry of the ligand field or to a Jahn−Teller effect.[28]

In the crystalline state, Cu(thiochrome)Cl_2 has a pseudotetrahedral coordination geometry with a dihedral angle of about 90.8° between the two coordination planes defined by the Cu−N−Cl moieties (see below). Generally pseudotetrahedral Cu(II) complexes are characterized by high $g_{||}$ values (2.25−2.40) and relatively low $A_{||}$ values (70−300 MHz).[29]

A linear anticorrelation between the values of $g_{||}$ and $A_{||}$ as a function of the degree of the tetrahedral distortion has been reported previously for structurally well-characterized Cu(II) complexes.[30] However, this stereochemical factor is not the only one in determining the EPR parameters in Cu(II) complexes. Other mechanisms, like the symmetry-allowed admixture of 4p orbitals in the ground state,[31] covalency, and ligand spin−orbit coupling effects[32,33] have been invoked in order to explain the observed $g_{||}$ and $A_{||}$ values in planar and tetrahedral Cu complexes.

In Cu(phen)$_2$$Cl_2$ the unpaired electron is delocalized 5−10% on the chloride ligands, and this in conjunction with the large spin−orbit coupling of the chloride atom is the origin of the relatively high $g_{||}$ (2.30) and low $A_{||}$ (370 MHz) values.[33] By reference to Table 4 it is seen that these values are close to those found for the Cu(thiochrome)Cl_2 ($g_{||} = 2.31$ and $A_{||} =$ 380 MHz); furthermore, in both cases the Cu(II) atom is in a pseudotetrahedral ligand environment and is coordinated by two nitrogens and two chlorides. We consider thus that in the Cu(thiochrome)Cl_2 a mechanism similar to that observed in Cu(phen)$_2$$Cl_2$ is responsible for the observed EPR spectrum.

Although the crystallographic symmetry of the complex is not axial, the EPR spectrum has apparent axial character. This most probably is due to vibronic effects which average the g_x and g_y components.[34] We thus assume that the $g_{x,y}$ components lie at any direction on the average equatorial plane defined by the chlorine and nitrogen ligands.

The magnetic susceptibility of [Cu($C_{12}H_{13}N_4OS$)Cl_2]·CH_3-OH has been measured in the 2−300 K temperature range. The μ_{eff}/Cu variation (1.68−1.74 μ_B) in the whole temperature range is small, indicating the absence of magnetic interactions between the Cu(II) ions of adjacent molecules which behave as isolated paramagnets. As it is discussed below (X-ray crystal structure determination section), the [Cu($C_{12}H_{13}N_4OS$)Cl_2] units are linked together into infinite chains developing along *b* through Cu−N(1″) bonds (Figure 2), yielding a 6.96 Å distance between adjacent Cu(II) ions along a chain. The paramagnetic behavior evident from the thermal variation of the magnetic susceptibility of complex **1** indicates that the electronic delocalization through the fused aromatic rings of the ligands including the N(4′a), N(3′), and N(1′) donor atoms is not sufficient to mediate superexchange interactions between adjacent Cu(II) ions ∼7 Å apart along the chains.

2.1. ESEEM Spectra of Cu(thiochrome)Cl_2. Representative time-domain ESEEM spectra for the Cu^{II}(thiochrome)Cl_2 complex recorded at a series of τ values, i.e., the time delay between the first and the second pulses, are displayed in Figure 4. The spectra have been recorded at a magnetic field **H** = 3325 G which corresponds to the maximum intensity of the field-swept spectrum, which is displayed in the inset in Figure 4. ESEEM spectra were recorded at five different magnetic

(27) Abragam, A.; Bleaney, B. *Electron Paramagnetic Resonance of Transition Ions*; Clarendon Press: Oxford, U.K., 1970; pp 455−469.
(28) Pilbrow, J. R. *Transition ion, electron paramagnetic resonance*; Oxford University Press: Oxford, 1990.
(29) Bencini, A.; Gatteschi, D. *Trans. Met. Chem.* **1982**, *8*, 1.
(30) Yokoi, H.; Addison, A. W. *Inorg. Chem.* **1977**, *16*, 1341.
(31) Starnoff, M. *J. Chem. Phys.* **1965**, *42*, 3383.
(32) Hathaway, B. J. *Coord. Chem. Rev.* **1981**, *35*, 211.
(33) Bencini, A.; Gatteschi, D.; Zanchini, C. *J. Am. Chem. Soc.* **1980**, *102*, 5234.
(34) Kokoszka, G.; Karlin, K. D.; Padula, F.; Baranowski, J.; Goldstein, C. *Inorg. Chem.* **1984**, *23*, 4378. (b) Barducci, R.; Bencini, A.; Gatteschi, D. *Inorg. Chem.* **1977**, *16*, 2117. (c) Hathaway, B. I.; Billing, D. E. *Coord. Chem. Rev.* **1970**, *5*, 143.

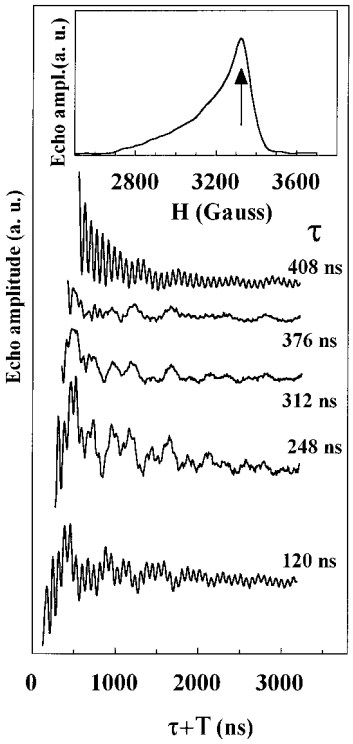

Figure 4. Stimulated-echo envelope modulation from the Cu(thiochrome)Cl_2 recorded at the indicated τ values. Inset: Echo-detected field-swept spectrum recorded with a two-pulse sequence. Experimental conditions: microwave frequency 9.6 GHz; magnetic field strength 3325 G; pulse sequence repetition rate 10 Hz; 15 events averaged/time point; temperature 12 K.

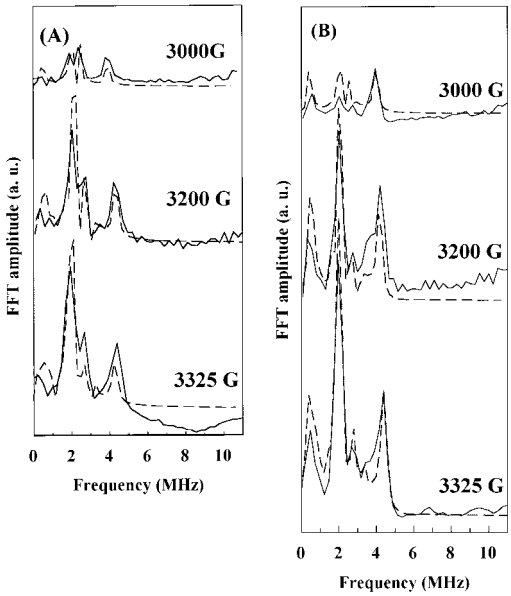

Figure 5. Fourier transformations of experimental (solid lines) and theoretical (dashed lines) ESEEM spectra for the Cu(thiochrome)Cl_2 complex for $\tau = 120$ ns (A) and 312 ns (B). In the calculations the tensor components listed in Table 6 were used for the three magnetic field strengths indicated in the figure. Experimental conditions as in Figure 4.

fields across the EPR line of the Cu(thiochrome)Cl_2. In Figure 5, solid lines display frequency-domain data for three magnetic field settings for $\tau = 120$ ns (5A) and 312 ns (5B), respectively. The major features found in the frequency-domain ESEEM spectra consist of two sharp lines near 2.0 and 2.9 MHz, a weaker one near 1.0 MHz, and an intense, relatively broader, line at 4.0−4.5 MHz.

ESEEM arises from weak magnetic couplings between the electron spin of Cu(II) and its surrounding nuclei.[35] From the X-ray structure, Figure 1, it is seen that the copper is coordinated by two nitrogens and two chlorides. The coupling of the directly coordinated nuclei, although not resolved in the CW EPR spectrum, is expected to be too large to give rise to envelope modulation.[19] This is a well-known phenomenon in copper complexes with nitrogenous ligands, as for example in Cu−imidazole complexes where the observed ESEEM arises from the remote, noncoordinated, nitrogen of the imidazole ring, while the coordinated nitrogen does not contribute to the observed modulation.[13,36] Therefore, as discussed below, the observed ESEEM for the Cu(thiochrome)Cl_2 is generated by the remote nitrogen N(3′) of the thiochrome ligand.

The best known case in ^{14}N-ESEEM spectroscopy is the "exact cancellation condition" where $|A_{iso}/2 - \upsilon_I| = 0$.[37] In this case, the three narrow low-frequency components arise from that ^{14}N superhyperfine spin manifold, where the nuclear−Zeeman and electron−nuclear hyperfine interactions approximately cancel one another, so that the level splittings are primarily determined by the ^{14}N nuclear quadrupole interaction (NQI).[37] In the case of exact cancellation, the ESEEM spectrum contains three sharp low-frequency lines, with maxima at frequencies given by the relations

$$\upsilon_+ = 3K(1+\eta), \quad \upsilon_- = 3K(1-\eta), \quad \upsilon_0 = 2K\eta \qquad (2)$$

where $K = e^2Qq_{zz}/4h$ is the quadrupole coupling constant, Q is the scalar quadrupole moment, $\eta = (q_{xx} - q_{yy})/q_{zz}$ is the asymmetry parameter of the electric field gradient $\{q_{ii}, i = x, y, z\}$ at the nucleus, and x, y, and z are the principal axes of the quadrupole coupling tensor.

The superhyperfine manifold, where the nuclear−Zeeman and the hyperfine interactions are additive, gives rise to much broader resonances,[35,37] and the only resolvable component is a double quantum transition line, $\Delta m_I = 2$, occurring at higher frequencies. The double-quantum line has maximum intensity at a frequency which is approximated by

$$\upsilon_{dq} \approx 2[(\upsilon_I + A/2)^2 + K^2(3+\eta^2)]^{1/2} \qquad (3)$$

where A is a secular component of the hyperfine coupling tensor determined mainly from its isotropic part.[37] According to expressions 2 and 3, within the cancellation condition, the peak positions υ_+, υ_-, and υ_0 are independent of the magnetic field, while the double-quantum line varies approximately as $\sim 2\cdot\Delta H\cdot\upsilon_I$. This field dependence is observed in the ESEEM spectra shown recorded at five magnetic field values, three of which are shown in Figure 5, indicating that the low-frequency features originate from ^{14}N-nuclear modulations. This is confirmed by detailed analysis by numerical simulations, see dashed lines in Figure 5, which are discussed in the following.

2.2. Simulations of the ESEEM Spectra. In the case of a deviation from the cancellation condition, the simple spectral features characterizing the exact cancellation are retained if the deviation is such that $\Delta < 4K/3\upsilon_I$,[37] and this allows, to a first approximation, an estimation of the nuclear quadrupole parameters K and η directly from the spectrum. In the present case we have used the values of K and η estimated in this way as starting values for the numerical simulation of the ESEEM spectra. The simulation procedure was directed toward the reproduction of the frequency positions of the main features,

(35) Dikanov, S. A.; Tsvetkov, Y. D.; Bowman, M. K.; Astashkin, A. V. *Chem. Phys. Lett.* **1982**, *90*, 149.
(36) Mims, W. B.; Peisach, J. *J. Chem. Phys.* **1978**, *69*, 4921.
(37) Flanagan, H. L.; Singel, D. J. *J. Chem. Phys.* **1987**, *87*, 5606.

Table 5. Range of Angles θ Selected at Each Field Position

magnetic field, G	2785	3000	3100	3200	3327
m_I(Cu)	$^3/_2$	$^1/_2$	$^3/_2$, $^1/_2$, $-^1/_2$	$-^1/_2$, $-^3/_2$	$-^3/_2$
θ range, deg	0−30	25−45	35−60	45−75	75−90

Table 6. Parameters Used for the Simulation of the ESEEM Spectra

$g_{xx} = g_{yy} = 2.06$	
$g_{zz} = 2.31$	
$A_{xx} = 1.6$ MHz	$a = 0°$
$A_{yy} = 1.4$ MHz	$b = 90°$
$A_{zz} = 1.0$ MHz	$c = 0°$
$e^2qQ/h = 4K = 3.1$ MHz	$u = 0°$
$\eta = 0.25$	$\upsilon = 90°$
	$w = 90°$

and in the following, the Euler angles were adjusted in order to simulate the relative intensity of the peaks. The simulations were performed at five magnetic field settings and for six τ values at each magnetic field. The errors associated with the various parameters are of the order of 10% while for the Euler angles the error is about 15°. The angles α, γ, and u have no effect on the simulated spectra and are set arbitrarily equal to 0.

In Table 5 we list the θ angles contributing to the total EPR spectrum at each magnetic field setting, for each of the four m_I ($+^3/_2$, $+^1/_2$, $-^1/_2$, $-^3/_2$) Cu(II) states. These angles were calculated for $\phi = 0$, and assuming that a range of 40 G contributes to the observed echo at each **H**. The simulated ESEEM spectra are shown by dashed lines in Figure 5, and the simulation parameters are summarized in Table 6.

In the present case the form of the hyperfine coupling tensor is essentially axial and can be put in the form ($A_{iso} - T$, $A_{iso} - T$, $A_{iso} + 2T$) with an anisotropic component of $T = -0.17$ MHz, which suggests that the electron−nuclear anisotropic interaction can be described by the point−dipole model. If we consider that the copper spin is located at a single point, then the anisotropic coupling of 0.17 MHz corresponds to an effective electron−nuclear distance of 3.5 Å. Alternatively we may consider the copper electron to be represented by four points with 0.25 spin density at each point. By putting the points at the four edges of the lobes of a $d_{x^2-y^2}$ orbital and the nucleus located perpendicular to the *xy*-orbital plane at a distance r_{eff} on the symmetry axis, one finds $r_{eff} = 2.2$ Å. The only nitrogen within the distance range limited by the two estimations of 3.5 and 2.2 Å is the N(3′) nitrogen of the pyrimidine ring. On this basis we assign the observed modulation to the coupling of the copper electron spin with the N(3′) nitrogen of the pyrimidine ring.

The isotropic coupling of $A_{iso} = 1.33$ MHz falls within the range of the isotropic couplings observed previously for the noncoordinated nitrogen of copper−imidazole complexes.[38] More specifically in bis(1,2-dimethylimidazole)copper(II) dichloride an A_{iso} of 1.45 MHz and an axial anisotropic hyperfine tensor with $T = 0.65$ MHz has been reported. In that complex, the copper atom is in a distorted tetrahedral coordination environment and the unpaired orbital is considered to be mainly $d_{x^2-y^2}$ as in the present case.

The isotropic hyperfine coupling between the copper and the N(3′) nitrogen of the pyrimidine ring implies the existence of an unpaired spin density on the nitrogen nucleus. This unpaired electron density could migrate in the pyrimidine π system by delocalization through the σ bond formed between the one lobe of the Cu(II) $d_{x^2-y^2}$ orbital and the sp^2 orbital of the directly coordinating nitrogen N(4′a) of the thiochrome ligand. On the basis of previous studies on crystalline pyrimidine in the triplet state,[39] a A_{iso} of 1.33 MHz may arise from a π spin density of 0.0012 at the nitrogen nucleus.

The copper unpaired electron is expected to have a significant impact on the ^{14}N hyperfine interaction. A correlation had been previously found between the magnitude of the nitrogen isotropic coupling from N donors directly bound to Cu(II) and the degree of tetrahedral distortion of the complex, i.e., the greater the deviation from square planar, the smaller the isotropic coupling.[40] As was pointed out in this earlier study, the amount of the overlap between the unpaired spin-occupied $d_{x^2-y^2}$ copper orbital and the directly coordinating nitrogen σ orbital decreases as the distortion increases and this then is reflected in a smaller nitrogen coupling. The contention that the ligand geometry may affect the nature of spin delocalization in a predictable manner is supported by single-crystal EPR studies on $Cu^{II}(Cl)_4$ in planar versus tetrahedral geometries.[41] An analogous correlation has been invoked for copper−imidazole compounds where a tetrahedral geometry decreases spin density on the coordinating σ orbital, at the same time increasing delocalization either into the ring π or C−N bond orbitals.[38] Both of these hybrid orbitals have considerably decreased s character, and this in turn results in a decreased nitrogen isotropic hyperfine coupling.

The principal directions of the quadrupole tensor Q_{xx}, Q_{yy}, and Q_{zz} are correlated with the directions of the valence-shell orbitals of ^{14}N. In crystalline pyrimidine the direction of Q_{zz} as determined by nuclear quadrupole resonance studies is perpendicular to the pyrimidine plane while the Q_{yy} axis lies along the bisector of the C−N(3′)−C angle.[42] The Q value found in the present case for the N(3′) nitrogen of the pyrimidine (3.1 MHz) is decreased in comparison with Q values (4.2−4.6 MHz) observed by NQR studies in crystalline pyrimidine. According to the Towens−Dailey model,[43] the change of the electric field gradient at a quadrupolar nucleus, such as ^{14}N, is attributed mainly to electrons in the valence shell p orbitals of that atom. In Cu(thiochrome)Cl_2 the participation of the pyrimidine ring in the thiochrome moiety together with the coordination to copper produces a change of the electron distribution in the molecular orbitals of the pyrimidine and, therefore, a change in the electron occupancy in the valence shell p orbitals of the N(3′) nitrogen. For this nitrogen each of the three sp^2-hybridized orbitals contains one valence electron. Two of these orbitals form σ bonds with the ring carbons, and the third sp^2 orbital is occupied by the nitrogen lone-pair electrons. The remaining p orbital participates in π bonding with the adjacent carbon atoms, forming a π molecular orbital in which the aromatic electrons are largely delocalized.[44] Within this context the decreased η value indicates a decreased difference between the π population and the average σ population. This change might be due to coordination to copper; in sp^2 hybrid nitrogens a reduction of e^2qQ up to 30% has been reported upon coordination to metals through the nitrogen lone pair orbital. These examples include zinc−imidazole, copper−imidazole,[45] and glyoxime−copper compounds.[46] When the

(38) Colaneri, M. J.; Potenza, J. A.; Schugar, H. J.; Peisach, J. *J. Am. Chem. Soc.* **1990**, *112*, 9451.
(39) Donckers, M. C. J. M.; Gorcester, J.; Schmidt, J. *J. Chem. Phys.* **1992**, *97*, 99.
(40) Iwaizumi, M.; Kudo, T.; Kita, S. *Inorg. Chem.* **1986**, *25*, 1546.
(41) Deeth, R. J.; Hitchman, M. A.; Lehmann, G.; Sachs, H. *Inorg. Chem.* **1984**, *23*, 1310.
(42) Shemb, E.; Bray, P. J. *J. Magn. Reson.* **1971**, *5*, 78.
(43) Towens, C. H.; Dailey, B. P. *J. Chem. Phys.* **1949**, *17*, 782.
(44) Shempb, E.; Bray, P. J. *J. Chem. Phys.* **1967**, *46*, 1186.
(45) Ashby C. I. H.; Paton, W. F.; Brown, T. L. *J. Am. Chem. Soc.* **1980**, *102*, 2990.
(46) Hsieh, Y.-N.; Ireland, P. S.; Brown, T. L. *J. Magn. Reson.* **1976**, *21*, 445.

nitrogen lone pair is perturbed, such as by coordination to a metal ion, a decrease of the electron population occurs and a decrease of e^2qQ would be expected.[45,46] In the present case the observed N(3′)−Cu distance is large (2.8 Å), and this precludes a strong bond between the N(3′) and the copper; it is likely that the copper−N(3′) interaction cannot fully account for the observed reduction of the e^2qQ value. A geometric alteration of the pyrimidine ring could also result in changes in the quadrupole coupling constants; the angle C(4′)−N(3′)−C(2′) in Cu(thiochrome)Cl_2 is 117.2° (Table 3), somewhat higher than the value of 115.5° observed in crystalline pyrimidine. According to studies on crystalline pyrimidine, such an increase implies a rehybridization of the nitrogen atomic orbitals, i.e., deviating from a pure sp^2 hybridization[39] toward a decrease in the s character mixing. In the pyrimidine triplet state this rehybridization is accompanied by a decrease of the quadrupole coupling constant. Within this context it is possible that the observed deviation of the C(4′)−N(3′)−C(2′) angle from 115.5° in the Cu^{II}(thiochrome)Cl_2 complex contributes to the observed reduction of the e^2qQ value.

3. Structure of {Cu(thiochrome)Cl_2}$_n$. An ORTEP diagram of complex **1** is shown in Figure 1 and the unit cell diagram in Figure 2. Bond distances and angles are presented in Table 3. The structure comprises an infinite array of Cu(thiochrome)Cl_2 neutral units linked together along the *b* direction through the N(4′a) and N(1′) atoms of the thiochrome molecule, which behaves as a bidentate bridging ligand. The Cu atom is in a flattened tetrahedral environment with two N atoms from different thiochrome molecules and two terminal Cl atoms. The distorted tetrahedra are clearly compressed along an S_4 axis [$2q = 152.3° \pm 5°$ (2×), $93.1° \pm 1°$ (4×)],[47] and this distortion is considerably higher than that observed in the structure of [(protonated thiamine)$^{2+}$($CuCl_4$)$^{2-}$] for the tetrachlorocuprate tetrahedron [$2q = 133.8° \pm 2.5°$ (2×), $99° \pm 1°$ (4×)].[5] The distortions of the molecule from D_{2d} symmetry are conveniently discussed by specifying three angles θ_x, θ_y, and θ_z. These angles refer to the orientation of the triangle with vertices Cl(1), Cu, Cl(2), relative to that of the corresponding triangle N(4′a), Cu, N(1″) (Figure 1). θ_z is generally similar to the dihedral angle between ligand planes usually reported for these structures. For molecules adopting D_{2d} symmetry, $\theta_x = \theta_y = \theta_z = 90°$. Deviation of θ_z from 90° represents a "twisting" of the second triangle N(4′a)CuN(1″) relative to the first one Cl(1)CuCl(2) and lowers the symmetry to D_2. The extreme case of this distortion is the "square planar" configuration (D_{2h} symmetry) for which $\theta_z = 0°$. Application of standard vector algebra techniques allows the calculation of θ_x, θ_y, and θ_z from the six N−Cu−N, Cl−Cu−Cl, and Cl−Cu−N angles usually reported.[48] The results of these calculations are $\theta_x = 90.2°$, $\theta_y = 87.0°$, and $\theta_z = 91.7°$, representing a slight deviation from D_{2d} symmetry. $\theta_z = 91.7°$ is in good agreement with the observed dihedral angles of 90.8° between both the N_2Cu and Cl_2Cu planes.

The metal ion is bonded to the N(1″) atom of the pyrimidine ring of thiochrome, as has been previously observed in numerous thiamine metal complexes,[2,3,6ab,49] and to the N(4′a) atom from another thiochrome molecule. The Cu−N (1.977 and 2.004 Å) and the terminal Cu−Cl (2.216 and 2.267 Å) bond distances are normal and comparable to values of "pyridine"-type complexes with a {CuN_2Cl_2} chromophore.[50] The Cu···N(3′) distance of 2.753 Å is significantly longer than the previous four distances. According to the ESEEM data the Cu···N(3′) isotropic hyperfine coupling is $A_{iso} = 1.33$ MHz, and this corresponds to a very small electron spin density (0.0012) transferred from the Cu(II) on the N(3′) nucleus. This shows that the Cu···N(3′) interaction is very weak and that N(3′) is not a ligand of the copper atom.

The C(4′)−N(4′a) bond distance of 1.363 Å (Table 3, Figure 1) is one of the longest found in crystal structures of metal thiamine complexes[49] and is due to the Cu(II)−N(4′a) coordination. It was suggested[6a] that the C(4′)−N(4′a)H_2 bond lengths (structure **I**), in addition to the C(2′)−N(1′)−C(6′) angle values (structure **I**), may depend linearly on the Lewis acid strength of the metallic ions in metal thiamine complexes with M−N(1′) bonding. Such a trend does not seem to be true;[49] however, we report here that the C(2′)−N(1′)−C(6′) angle of 117.6° (Table 3) in the present structure is the largest found in crystal structures of metal thiamine complexes with a direct M−N(1′) bond.

The crystal structure of {Cu^{I}_2(thiochrome)$_2$(ClO_4)$_2$}$_n$[6c] shows substantial differences when compared with the crystal structure reported here: (i) the copper ion occurs in the +1 oxidation state and has a three-coordinate T-shaped geometry with two nitrogen donors and one oxygen donor; (ii) the binuclear copper units [Cu_2(thiochrome)$_2$]$^{2+}$ are positively charged, and the structure is described as infinite polycation chains with anion columns along these chains; (iii) the dimeric units are linked by the hydroxyl group of the coordinated thiochrome and each copper (I) in the unit is bonded to the N(3′) atom from the first thiochrome and to the N(4′a) atom from the second thiochrome molecule.

Although there is a difference in the oxidation state of copper ion, its binding sites, and the mode of polymerization between the {Cu_2(thiochrome)$_2$(ClO_4)$_2$}$_n$ and the title compound, there is little difference in bond distances and angles of the thiochrome molecules. The difference observed in the C(2′)−N(3′) bond distance [1.328 (Table 3) and 1.364 Å for the present structure and for {Cu_2(thiochrome)$_2$(ClO_4)$_2$}$_n$, respectively] is expected since the N(3′) is coordinated to the copper atom only in the latter structure.

In examining the factors which determine the crystal structure, we emphasize the following. (i) *The nature and size of the counterion:* Small chloride anions able to coordinate to the metal could lead to neutral Cu(thiochrome)Cl_2 units, in contrast to bulky, rarely coordinated[51] perchlorate anions which could drive in dimeric charged [Cu_2(thiochrome)$_2$]$^{2+}$ units with no anion coordination. (ii) *The method of crystal preparation (type and complexity of the reaction):* While the ligand reagent used to synthesize the title compound consisted of 2-(α-hydroxybenzyl)-thiamine, the crystal structure of the product suggests thiochrome. Thus, the formation of crystals of a Cu(II)−thiochrome complex indicates that redox reaction has occurred. 2-(α-hydroxybenzyl)thiamine has been oxidized to thiochrome, and some of the bivalent copper has been reduced.

Biological Implications. The present data show that the reaction of Cu(II) with 2-(α-hydroxybenzyl)thiamine in solution produces Cu(I) and thiochrome:

(47) Smith, D. W. *Coord. Chem. Rev.* **1976**, *21*, 93. (b) Reinen, D. *Comments Inorg. Chem.* **1983**, *2* (5), 227.
(48) Dobson, J. F.; Green, B. E.; Healy, P. C.; Kennard, C. H. L.; Pakawatchai, C.; White, A. H. *Aust. J. Chem.* **1984**, *37*, 649. (b) Knapp, S.; Keenan, T. P.; Zhang, X.; Fikar, R.; Potenza, J. A.; Schugar, H. J. *J. Am. Chem. Soc.* **1990**, *112*, 3452.
(49) Louloudi, M.; Hadjiliadis, N. *Coord. Chem. Rev.* **1994**, *135*, 429.
(50) Mosset, A.; Tuchagues, J. P.; Bonnet, J. J.; Haran, R.; Sharrock, P. *Inorg. Chem.* **1980**, *19*, 290. (b) van Ooijen, J. A. C.; Reedijk, J.; Spek, A. L. *J. Chem. Soc., Dalton Trans.* **1979**, 1183.
(51) Rosenthal, M. R. *J. Chem. Educ.* **1973**, *50*, 331.

$$\underset{\text{2-(}\alpha\text{-hydroxybenzyl)thiamine}}{C_{19}N_4O_2SH_{23}Cl} + 3Cu^{II}Cl_2 \rightarrow Cu^{II}(C_{12}N_4OSH_{14})Cl_2 + 2Cu^{I}Cl + 3HCl + C_6H_5CHO$$
$$\underset{Cu^{II}\text{(thiochrome)}Cl_2}{}$$

The X-ray, EPR and magnetic susceptibility data show that the thiochrome is coordinated to Cu(II), which most likely comes from remaining amounts of Cu(II) reagent.

A similar reaction has been reported to occur with Cu(II) and thiamine:[6a]

$$2Cu^{II} + \underset{\text{thiamine hydrochloride}}{3C_{12}N_4OSH_{18}Cl_2} \rightarrow \underset{Cu^{I}\text{(thiamine)}Cl_2}{2Cu^{I}(C_{12}N_4OSH_{17})Cl_2} + \underset{\text{thiochrome}}{C_{12}N_4OSH_{14}} + 2Cl^- + 6H^+$$

It is thus seen that in solution the reaction of Cu(II) with either thiamine or one of its intermediate "active aldehyde" derivatives results in their oxidation to thiochrome. In living organisms the formation of thiochrome would inhibit the normal enzymatic action of thiamine. With the data at hand, we cannot determine the mechanism which apparently has to operate *in vivo* in order to prevent thiochrome formation due to the reaction of thiamine with the abundant Cu(II) ions. In this context it is important to examine whether or not the reaction of Cu(II) with the α-(hydroxyethyl)thiamine pyrophosphate derivative, which is the active intermediate of the enzymatic cycle of thiamine *in vivo*, leads to thiochrome formation. Experiments in this direction are currently in progress in our lab.

Conclusion

The crystal structure of the Cu^{II}(thiochrome)Cl_2 complex shows that the copper atom is tetracoordinated with a Cu···N-(3′) weak interaction in a compressed tetrahedral environment. Values of θ angles show that it approximates D_{2d} symmetry within a few degrees.

In the Cu^{II}(thiochrome)Cl_2 the magnetic interaction between the N(3′) nitrogen of the pyrimidine ring and the copper $d_{x^2-y^2}$ electron spin is detected by ESEEM spectroscopy. The ESEEM study reveals the existence of a small percentage of unpaired spin density on the N(3′) nitrogen. The electron distribution on the pyrimidine ring in Cu^{II}(thiochrome)Cl_2 differs substantially from that in crystalline pyrimidine as indicated from the quadrupole parameters ($e^2qQ = 3.1$ MHz, $\eta = 0.25$). The CW and pulsed EPR data provide structural information which is in agreement with the crystal structure, and this fact indicates once more[12,13] that these techniques can provide reliable information for the study of the coordination enviroment of copper(II) in biological systems, metalloproteins, and other systems, in the absence of X-ray diffraction data.

The understanding of when Cu(II) does or does not oxidizes thiamine and the intermediates of its enzymatic cycle in biological systems is of great importance, and more work is needed to elucidate thiamine oxidation in the presence of Cu-(II) ions.

Supporting Information Available: Table S1 with crystal data, data collection, and refinement parameters, Table S2 with fractional atomic coordinates and isotropic thermal parameters for hydrogen atoms, Table S3 with anisotropic thermal parameters, Table S4 with the magnetic susceptibility measurements for complex **1** in the 300−2 K temperature range, and one figure with the angle-dependent Cu(II) EPR spectrum (5 pages). Ordering information is given on any current masthead page.

IC970638K